Loran Tomography

Nobuyoshi Kouguchi

Kobe University of Mercantile Marine
Fukae-minamimachi 5-1-1, Higashinada-ku, Kobe-city, 658, JAPAN
E-mail:kouguchi@cc.kshosen.ac.jp

International Loran Association 30th Annual Convention and Technical Symposium
St. Germain-en-Laye, France
October 7-10, 2001

Abstract

The term of tomography is usually used for the oceanic engineering, seismology and medical applications, which is to infer the characteristics of the propagation path from precise measurement of time of arrival (TOA). To apply for Loran system, the time of arrival is function of the conductivity and irregularity of the propagation surface. Then it is considered that the propagation profile in any Loran chain can be inferred from the TOA and other information (pulse distortion). This is the inverse problem of tomography. In this paper, first the system structure of Loran tomography is discussed, next the Loran tomography formula and method by means of the precise information of TOA is shown and last a feasibility and effectiveness about Loran tomography is described.

1 Introduction

Loran-C receivers measure the Time Differences (Distance Difference) from the transmitter to receiver and fix their position as a intersection of these hyperbolas. To convert the time to distance, Loran receivers make use of temporary propagation speed over the seawater. Then the temporary speed is different from the actual signal speed. he deviation of time difference due to this difference is called as ASFs (Additionary Secondary Factors).

In present Loran system, it is well known that the Loran repeatable accuracy is better than 80 [m] (2DRMs), but the absolute accuracy might be as poor as 500 to 1000 [m]. To improve the absolute accuracy up to repeatable one, we should use the actual propagation speed and ASF correction. On this correction, there are three methods. The first method is using the ASF correction table [1] [2], which had been calculated the ASF value. The second method is using calibrated data that had been compared with GPS positions. The third method is using the pulse distortion measures [3] [4] [5] [6] that are distorted due to the characteristics of propagation path.

Ocean Acoustic Tomography, proposed by Munk and Munsch in 1979, is a useful and conventional tool to infer the state of the ocean traversed by the sound field [7]. The technology of tomography is also one attractive and efficient method for the Loran ASF correction, because we could construct precise ASFs map by only one observation flight or voyage around the evaluation area.

In this paper, we propose the Loran Tomography, and describe the technique that is used to construct ASFs maps at the example area near Japan Sea. A feasibility of Loran Tomography was evaluated using three tomographic inversion ASFs maps.

2 Statistical inversion [9]

ASFs were defined as the additional phase shift relative to an all seawater path caused by the overland portion of the propagation path [2]. The difference between the temporal propagation speed and actual signal speed is divided into two parts. One is $C_{seawater}$ (SF: Secondary Factor) the speed over seawater and the other is the perturbation term $\Delta C(x,y)$ (ASF) that depend on the characteristics of propagation path. Then the actual propagation speed of Loran signal is C, then

$$\begin{aligned} C &= SF + ASF \\ &= C_{seawater} + \Delta C(x,y) \end{aligned} \tag{1}$$

where (x, y) are the horizontal coordinate on the earth, and $C_{seawater} >> \Delta C(x,y)$. The propagation time of Loran signal from a transmitter to receiver can be expressed by

$$\tau = \int_{transmitter}^{receiver} \frac{dr}{C} = \int_{\Gamma} \frac{dr}{C} \tag{2}$$

$$\tau_{seawater} = \int_{\Gamma_{seawater}} \frac{dr}{C_{seawater}} \tag{3}$$

where Γ and $\Gamma_{seawater}$ are propagation paths for C and $C_{seawater}$ respectively, r is a distance measured from a transmitter to receiver.

The approximation $\Gamma \approx \Gamma_{seawater}$ is leading to follow approximation.

$$\begin{aligned} \Delta\tau &= \tau - \tau_{seawater} \\ &= \int_{\Gamma} \frac{dr}{C_{seawater} + \Delta C} - \int_{\Gamma_{seawater}} \frac{dr}{C_{seawater}} \\ &\approx -\int_{\Gamma_{seawater}} \frac{\Delta C}{C_s^2} \end{aligned} \tag{4}$$

Converting above equation to discrete formula, Eq.(4) can be written

$$\Delta\tau_i = \sum_{j=1}^{N} G_{ij}\Delta C_j \quad (i = 1, 2, \cdots, M) \tag{5}$$

for all propagation paths, where M and N denote the numbers of the propagation paths and rectangular cells, respectively. In Eq.(5), $G_{ij} = -\frac{R_{ij}}{C_{sj}^2}$ and R_{ij} is a length of the i'th propagation path crossing the j'th cell (see Fig.1). By using a vector and matrix notation, Eq. (5) is rewritten as,

$$\Delta\tau = \mathbf{G}\Delta\mathbf{C} \tag{6}$$

where $\Delta\tau = \Delta t_i$, $\Delta\mathbf{C} = \Delta C_j$ and $\mathbf{G} = G_{ij}$. For square matrix $\mathbf{G}$, the conventional inverse is

$$\widehat{\Delta\mathbf{C}} = \mathbf{G}^{-1}\Delta\tau \tag{7}$$

In above equation, $\widehat{\Delta\mathbf{C}}$ is the estimate of $\Delta\mathbf{C}$.

In consideration of the error $\mathbf{n}$ that is introduced to

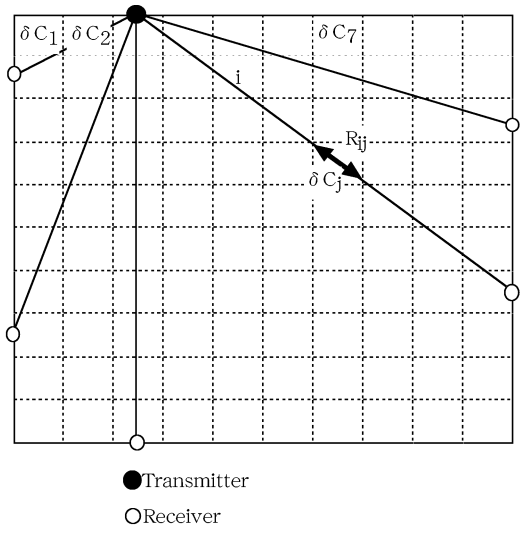

Figure 1: Tomography Configuration

represent both the noise component of $\Delta\tau$ and error resulting from the liberalization, Eq.(7) is transformed into

$$\Delta\tau = \mathbf{G}\Delta\mathbf{C} + \mathbf{n} \tag{8}$$

where $\mathbf{n} = \{n_i\}$.

An error $\mathbf{e}$ is a difference between the true value $\Delta\mathbf{C}$ and estimate $\widehat{\Delta\mathbf{C}}$;

$$\mathbf{e} = \widehat{\Delta\mathbf{C}} - \Delta\mathbf{C} \tag{9}$$

The covariance matrix $\mathbf{C}_e$ of $\mathbf{e}$ may be defined as

$$\begin{aligned} \mathbf{C}_e &= \langle \mathbf{e} \cdot \mathbf{e}^T \rangle \\ &= \langle (\widehat{\Delta\mathbf{C}} - \Delta\mathbf{C}) \cdot (\widehat{\Delta\mathbf{C}} - \Delta\mathbf{C})^T \rangle \end{aligned} \tag{10}$$

where $<>$ denotes the ensemble mean and the superscript T denotes the transpose of the matrix.

If the number of propagation paths M is larger than the number of rectangular cells N, Least Square

Method is used and we can use a set of normal equation with solution,

$$\widehat{\Delta \mathbf{C}} = (\mathbf{G}^T\mathbf{G})^{-1}\mathbf{G}^T\Delta\tau \tag{11}$$

From the condition that makes $\mathbf{C}_e$ minimum, operator $\mathbf{L}$ can be determined as follows:

$$\widehat{\Delta \mathbf{C}} = \mathbf{C}_{\Delta C}\mathbf{G}^T(\mathbf{G}\mathbf{C}_{\Delta C}\mathbf{G}^T + \mathbf{C}_n)^{-1}\Delta\tau \tag{12}$$

where $\mathbf{C}_{\Delta C}$ and $\mathbf{C}_n$ are the covariance matrices for $\Delta\mathbf{C}$ and $\mathbf{n}$, respectively.

Let us assume here that all the components of $\mathbf{C}_{\Delta C}$ and $\mathbf{C}_n$ possess the following constant values $\sigma^2_{\Delta C}$ and σ^2_n respectively:

$$\begin{aligned} \mathbf{C}_{\Delta C} &= \sigma^2_{\Delta C}\mathbf{I}_M \\ \mathbf{C}_n &= \sigma^2_n\mathbf{I}_M \end{aligned} \tag{13}$$

where $\mathbf{I}_M$ is the $M \times M$ unit matrix.

According to the singular value decomposition (SVD) method, $\mathbf{G}$ can be expressed by

$$\mathbf{G} = \mathbf{U}_M\mathbf{\Lambda}\mathbf{V}_N^T \tag{14}$$

where $\mathbf{U}_M$ and $\mathbf{V}_N$ are the matrices constructed from the non-zero eigenvectors of Hermitian matrices $\mathbf{G}\mathbf{G}^T$ and $\mathbf{G}^T\mathbf{G}$, respectively [8]. Furthermore $\mathbf{\Lambda}$ as the number $M \times N$ matrix whose diagonal elements are λ_i are composed of the non-zero singular value of $\mathbf{G}\mathbf{G}^T$ or $\mathbf{G}^T\mathbf{G}$. The subscript M is the number of the propagation paths, and also the number of the non-zero singular values. N is the number of the rectangular cells and also equal to the rank of $\mathbf{G}$. Putting $\alpha^2 = \frac{\Delta_n^2}{\Delta_{C\Delta^2}}$ and substituting Eq.(13) and (14) into Eq.(12), finally we can obtain

$$\widehat{\Delta \mathbf{C}} = \mathbf{V}_N\mathbf{\Lambda}\mathbf{\Lambda}^T(\mathbf{\Lambda}\mathbf{\Lambda}^T + \alpha^2\mathbf{I}_M)^{-1}\mathbf{U}_M^T\Delta\tau \tag{15}$$

3 Numerical experiment

3.1 Loran tomography configurations

Some numerical experiments are carried out as an illustration of near Japan Sea. The size of experimental area is surrounded by the latitude lines from 34 ° N to 43 ° N and the longitude lines from 129 ° E to 145 ° E. This area is divided of 0.5 ° N × 0.5 ° E, then there are 540 rectangular cells. In this area, three actual transmitter stations (Niijima, Tokatibuto, Pohang) were set. Fig.2 illustrates the Loran Tomography configuration near Japan Sea as an example of 31 receiver points. For model simplification, following conditions

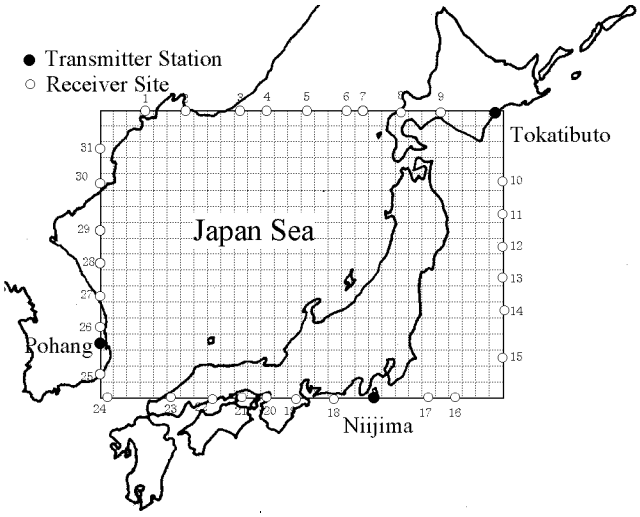

Figure 2: Loran Tomography Configuration (Japan Sea)

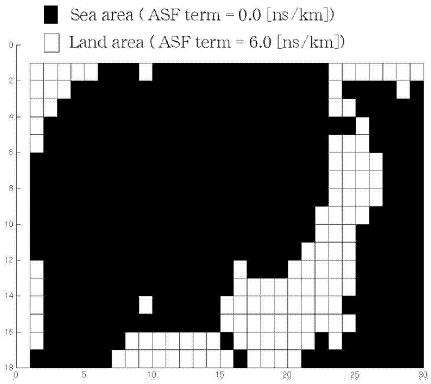

Figure 3: ASFs map

are assumed for after experiment,

1. Each cell has the uniformly distributed ASF value.

2. The shape of cell is a square (60 × 60 $[km^2]$).

In Fig.2, each cell is allocated two ASF values that are the seawater ($\Delta C = 0.0$ [ns/km]) and land ($\Delta C = 0.6$ [ns/km]) [10]. ASFs map near Japan Sea is shown in Fig.3. In this figure, white rectangular cell means the sea area and black cell means the land area.

3.2 Evaluation figures

The deviations of propagation time can be shown as the linear combinations of ASF value in each cells, and the problem to estimate ASF distribution results in solving simultaneous linear equations in Algebra. Also an estimated accuracy and resolution of tomography depend on the number of divided cell, configuration of transmitters and receivers, measurement accuracy of time and etc. However there are many kinds of evaluating figure of tomography, in this study the correlation coefficient between actual ASFs value and estimated ASFs in all evaluation cells was defined as follows [8];

$$\rho = \frac{\sum_{i=1}^{N} \Delta C_i \widehat{\Delta C_i}}{\sqrt{\sum_{i=1}^{N} {\Delta C_i}^2} \sqrt{\sum_{i=1}^{N} {\widehat{\Delta C_i}}^2}} \tag{16}$$

where the superscript i denotes the order of cells and N the number of the ell in tomography map.

We use one more reference figure[8] which is the spatial resolution. If propagation paths are uniformly distributed, following equation is set up a standard to estimate the resolution length (ΔR).

$$\Delta R = \sqrt{\frac{A}{M}} \tag{17}$$

where A is the area size of the tomography site, M is the number of the propagation paths.

3.3 Experimental results

In this experiment, three kinds of receiver configurations are used to evaluate a feasibility for ASFs map by means of the tomography. Fig.4, 6 and Fig.8 show the results of this experiment, and each figure has different number of receiver points. Fig.5, Fig.7 and Fig.9 are binarized results of Fig.4, Fig.6 and Fig.8 respectively. First two results, all receiver points are allocated on a boundary of the tomography map and the number of receiver points are selected 21 and 31 respectively. Third one has 41 receiver points are selected and it has five inside receiver points. If we have only one experimental voyage or flight around the evaluation area, a large number of receiver points are utilized. Then this ASFs map using tomography inversion has a good cost and time performance for making ASF maps.

Tab.1 shows the numerical results for three experiments. The number of receiver points becomes grater, the correlation coefficient become larger. From the viewpoints of Algebra, the rank of matrix $\mathbf{G}$ should be selected as same as the number of rectangular cells (N). In this experiment, all number of M that is as same as the rank of $\mathbf{G}$ are considerably fewer in order to numerical restrictions. Then it is consider that the proper number of receiver points could make a suitable resolution of ASFs map.

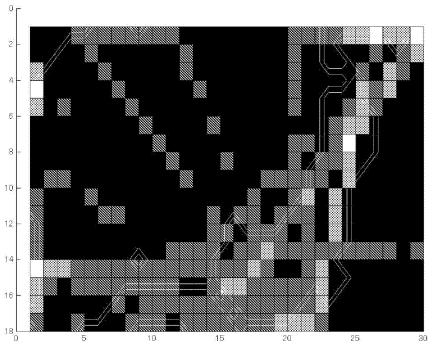

Figure 4: 4 steps ASFs map of 3 transmitter stations and 21 receivers (M=540, N=63)

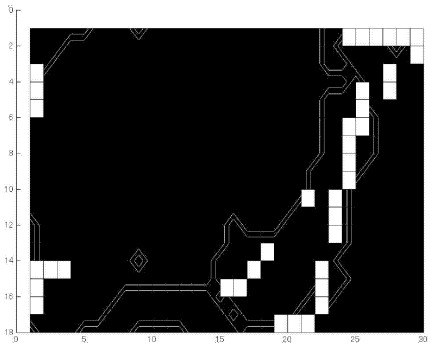

Figure 5: Binarized result of Fig.4

Table 1: Numerical results of experiment

Experimental No.	No. of transmitter site	No. of receiving point	M (No. of propagation path)	N (No. of rectangular cell)	rank($\mathbf{G}$)	ΔR [km]	ρ
1	3	21	63	540	63	175.7	0.48
2	3	31	93	540	93	144.6	0.63
3	3	41	123	540	123	125.7	0.68

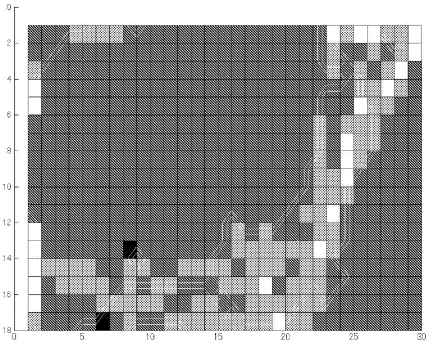

Figure 6: 4 steps ASFs map of 3 transmitter stations and 31 receivers (M=540, N=93)

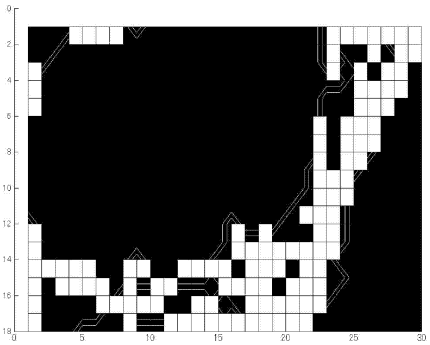

Figure 7: Binarized result of Fig.6

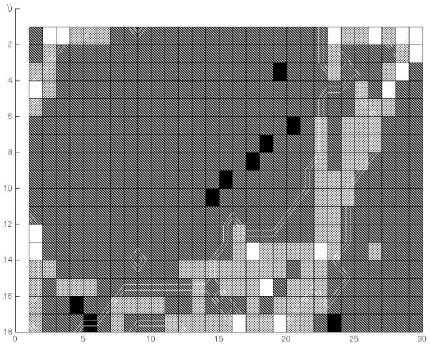

Figure 8: 4 steps ASFs map of 3 transmitter stations and 41 receivers (M=540, N=123)

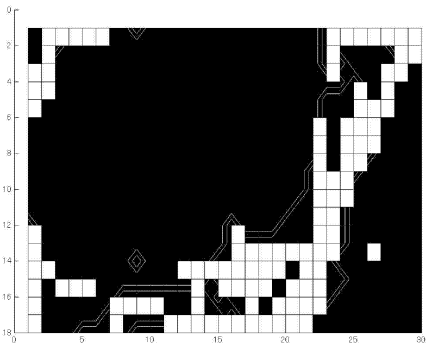

Figure 9: Binarized result of Fig.8

4 Conclusion

The loran tomography system was proposed and evaluated through the numerical experiments. Statistical inversion approach for tomography was applied to construct ASFs maps. Three receiver configurations were used to evaluate a feasibility of this method. If we have only one experimental voyage or flight around the evaluation area, a large number of receiver points are utilized. Consequently this ASFs map using tomography inversion had a good cost and time performance for constructing ASF maps. Also in this experimental area, more actual three transmitters (Ussuriisk (Russia), Kwangju (Republic of Korea) and Helong (China)) were existed. Then we will be able to have better the degree of resolution ASFs maps in future experiment.

Acknowledgement

The author wish to express my thankfulness to Dr. Iwao NAKANO Japan Marine Science and Technology Center and KOBE Univ. of Mercantile Marine Navigational Cybernetics Lab Research Group for many helpful suggestions and to staff of our lab.

References

[1] U.S. Naval Oceanographic Office: "Loran-C correction table"

[2] David Last, Paul Williams and Kenneth Dykstra, " Propagation of Loran-C Signal in Irregular Terrain Modelling and Measurements", Proceedings of the 29th Annual Technical Symposium, The International Loran Association,2000

[3] N.Kouguchi, M.Sato and N.Morinaga: "A Study of the Distortion and Propagation Time-Delay of Loran-C Pulse Wave Based on a Model of the Propagation Path", Proceedings of the 19th Annual Technical Symposium, Wild Goose Association,1990

[4] N.Kouguchi, M.Sato and N.Morinaga: "Measurement Technique for Loran-C Pulse Wave Distortion Measures and Performance in an Environment of Noise", Proceedings of IEEE PLANS'92, 1992

[5] N.Kouguchi, M.Sato and N.Morinaga: "Experimental Study on Loran-C Pulse Distortion", Proceedings of the 23rd Annual Technical Symposium, The International Loran Association,1994

[6] N.Kouguchi: "Distance Characteristics of Received Pulse wave Signal in Northwest Pacific Chain.", Proceedings of the 26th Annual Technical Symposium, The International Loran Association,1997

[7] Iwao Nakano, Shunji Ozaki, Gentaro Kai, Koki Midorikawa and Toshiyuki Nakanishi, " Optimal Configuration with Various Sources and Receivers for Ocean Acoustic Tomography", Japan Marine Science and Technology Center Report R, Vol.24, pp.269-285,1990

[8] Arata Kaneko, Gang Yuan, Noriaki Gohda and Iwao Nakano, " Optimum Design of the Ocean Acoustic Tomography System for the Sea of Japan", Journal of Oceanography, Vol.50, pp.281-293,1994

[9] Walter Munk, Peter Worcester and Carl Wunsch: "Ocean Acoustic Tomography", Cambridge University Press, 1995

[10] Fusakichi Ono and Kyozi Nagamori: "Estimation of the Land Effect on LORAN C Wave Propagation and Correction Chart",Navigation (Japan Institute of Navigation) ,No.85, 1985.

Biography

Nobuyoshi KKOUGUCHI was born in Okayama, Japan, in 1955. He received the B.Sc. degree in nautical science from Kobe University of Mercantile Marine 1978 and PhD in telecommunication engineering from Osaka University 1998.

From 1979 to 1991, he joined the Marine Technical College as a Research Associate and Associate Professor. Since 1991, he has been an Associate Professor at Kobe University of Mercantile Marine and from 1996 to 1997 he worked as a Captain of the Training ship. His research has focused on the evaluation of radio navigation system (especially Loran and GPS), radar signal processing, and the recognition of navigator.